*Chinese Journal of*
**POLYMER SCIENCE**

RESEARCH ARTICLE

https://doi.org/10.1007/s10118-024-3107-7
*Chinese J. Polym. Sci.* **2024**, *42*, 838–850

# Bilayer Compounded Polytetrafluoroethylene Membrane for Enhanced Oil-Water Emulsion Separation

Yu-Liang Yang[a], Tai-Ran Zhang[a], Yan-Ting Han[b], Shao-Yun Guo[a], Qin-Gong Rong[c], and Jia-Bin Shen[a*]

[a] *State Key Laboratory of Polymer Materials Engineering, Polymer Research Institute of Sichuan University, Sichuan Provincial Engineering Laboratory of Plastic/Rubber Complex Processing Technology, Chengdu 610065, China*
[b] *West China Hospital/West China School of Nursing, Sichuan University, Chengdu 610041, China*
[c] *Shandong Senrong New Materials Co., Ltd., Zibo 256401, China*

Electronic Supplementary Information

**Abstract** In order to achieve efficient and durable oil-water emulsion separation, the membranes possessing high separation efficiency and mechanical strength attract extensive attention and are in great demand. In present study, a kind of polytetrafluoroethylene (PTFE)-based bilayer membrane was fabricated by electrospinning fibrous PTFE (fPTFE) on an expanded PTFE (ePTFE) substrate. The morphological observation revealed that the fibrous structure of the fPTFE layer could be tailored by controlling the formulation of spinning solution. The addition of appropriate polyoxyethylene (PEO) would make the fibers in the fPTFE layer finer and more uniform. As a result, the compounded membrane exhibited a small pore size of approximately 1.25 μm and a substantial porosity nearing 80%. This led to super-hydrophobicity, characterized by a high water contact angle (WCA) of 149.8°, and facilitated rapid oil permeation. The water-in-oil emulsion separation experiment further confirmed that the compounded membrane not only had a high separation efficiency closing 100%, but such an outstanding separation capacity could be largely retained, either through multiple cycles of use or through strong acid (pH=1), strong alkali (pH=12), or high-temperature (100 °C) treatment. Additionally, the mechanical behavior of the bilayer membrane was basically contributed by that of each layer in terms of their volume ratio. More significantly, the poor creep resistance of fPTFE layer was suppressed by compounding with ePTFE substrate. Hence, this study has laid the groundwork for a novel approach to create PTFE-based compounded membranes with exceptional overall characteristics, showing promise for applications in the realm of emulsion separation.

**Keywords** ePTFE; Electrospinning membrane; Bilayer compounding; Emulsion separation

**Citation:** Yang, Y. L.; Zhang, T. R.; Han, Y. T.; Guo, S. Y.; Rong, Q. G.; Shen, J. B. Bilayer compounded polytetrafluoroethylene membrane for enhanced oil-water emulsion separation. *Chinese J. Polym. Sci.* **2024**, *42*, 838–850.

## INTRODUCTION

With the rapid development of the chemical industry, a substantial volume of oily wastewater inevitably emerges during the production processes, which damages the ecological environment.[1–4] The water and oil in oily sewage can form stable water-in-oil emulsion, presenting a formidable challenge in terms of separation.[5,6] Among various separation technologies, advanced functional membranes consisting of low surface energy polymeric matrix and tailored micropores exhibit characteristics of simplicity, high efficiency, and energy conservation, widely applied in the selective separation and purification of oily sewage.[7,8] However, many polymer materials are unable to withstand harsh conditions such as high temperatures and corrosive, limiting their practical applications. Polytetrafluoroethylene (PTFE) stands out as an ideal material for fabricating high-performance water-in-oil emulsion separation membranes, owing to its exceptional hydrophobic properties, high thermal stability, and resistance to corrosion.[9–11]

Besides the super wettability property, the porous structure of water-in-oil emulsion separation membranes is also crucial during the separation process.[12–14] The porous structure primarily includes pore size and porosity, which affect the separation efficiency and speed.[15,16] Larger pore or higher porosity can lead to faster separation speed. However, the enlargement of pore size can make smaller water droplets more prone to pass through the membrane, consequently leading to a reduction in separation efficiency. Therefore, designing separation membranes with both high porosity and appropriate pore sizes is highly desirable for achieving excellent separation efficiency.

Since PTFE resins are insoluble and difficult to be melt, traditional thermoplastic methods cannot be used for processing.[11] Currently, the typical methods for preparing PTFE oil-water separation membranes are electrospinning and thermal stretching.[17,18] Fibrous PTFE (fPTFE) membranes pro-

* Corresponding author, E-mail: shenjb@scu.edu.cn
Received December 21, 2023; Accepted February 22, 2024; Published online April 3, 2024

duced by electrospinning possess advantages of specific surface area and high porosity, thereby demonstrating outstanding separation efficiency in oil-water emulsion separation.[19] Importantly, the three-dimensional interweaving and layer-by-layer stacking of the fibers significantly enhance the membrane's porosity, altering its pore structure.[20] However, due to the smaller fiber diameter and the potential structural defects caused by sintering, the mechanical strength and ductility of the membrane may be compromised. Thermal stretching is usually employed to prepare expanded PTFE (ePTFE) membranes. Research indicates that the regulation of the porous structure primarily depends on the stretching rate.[21,22] A high stretching rate is favorable for achieving large pore, high porosity, and mechanical strength but inevitably result in decreased separation efficiency. Compared to fPTFE, ePTFE exhibits relatively lower porosity and smaller surface area but higher mechanical strength. From the perspective of practical applications, an ideal separation membrane not only possesses excellent separation efficiency but also has certain mechanical properties to ensure reliability and durability during usage.

To achieve more ideal performance goals, special methods are commonly employed to combine different materials, leveraging their complementary advantages.[23] A typical example involves combining PTFE membranes with thermoplastic polyurethane elastomers (TPU) using specific adhesives.[24,25] This layered compound structure fully utilizes the advantages of each material, resulting in improved elasticity and resistance to creep deformation. Therefore, it is of paramount importance to conceive and fabricate an ideal structure, ensuring that the water-in-oil emulsion separation membrane attains optimal comprehensive performance.

In order to utilize the advantages of ePTFE and fPTFE and compensate for their respective shortcomings, this study adopts an innovative approach by electrospinning a PTFE emulsion onto an ePTFE membrane, creating an ePTFE/fPTFE bilayer compounded membrane. Through precise control of the formulation, the fiber structure of the fPTFE layer was tailored, and the pore structure of the membrane was regulated. The morphology, separation performance, and mechanical property of the compounded membrane were measured and investigated. It was demonstrated that such a structural combination strategy endowed the hierarchical membrane with high mechanical strength of ePTFE membrane and the high separation efficiency of fPTFE membrane, which paved a new way to fabricate high-performance separation membranes.

## EXPERIMENTAL

### Materials

Commercial PTFE aqueous dispersion (sfn1, 60 wt%) was offered by Zhonghao Chenguang Research Institute (China). Poly(ethylene oxide) (PEO) was provided by Shanghai Mai Lin Biochemical Company (China) with a molecular weight of approximately $3\times10^5$ g/mol. ePTFE microporous membrane was provided by Shandong Senrong Company (China). These ePTFE membranes have a pore size of 1 μm and a porosity of 51%. Sodium hydroxide, chloroform and hydrochloric acid were obtained from Chengdu Kelong Chemical Reagent (China) without further purification.

### Membrane Preparation

The detailed mass ratios of the PTFE/PEO solutions used in the experiments are listed in Table 1. The PEO powders were prepared by dissolving the PEO powders in a PTFE aqueous dispersion and sonicated at 40 °C for at least 4 h.

**Table 1** Composition of electrospinning solutions.

| Membrane code | PEO (g) | PTFE aqueous dispersion (g) | $H_2O$ (g) | PTFE:PEO (g/g) |
|---|---|---|---|---|
| M1 | 1 | 6.67 | 8 | 4:1 |
| M2 | 1 | 16.67 | 8 | 10:1 |
| M3 | 1 | 26.67 | 8 | 16:1 |
| M4 | 1 | 36.67 | 8 | 22:1 |
| M5 | 1 | 46.67 | 8 | 28:1 |
| M6 | 1 | 56.67 | 8 | 34:1 |

The manufacturing process of the bilayer compounded membrane is shown schematically in Fig. 1. The configured PTFE/PEO solution was loaded into a syringe attached to a 16 G needle, which was used as a spinneret. A positive voltage was applied to the needle, while a negative voltage was applied to the negative electrode. The ePTFE membrane attached to a piece of polyimide (PI) film was placed on the collector as a substrate. The PTFE/PEO nanofibers, referred to as fPTFE, were electrospun from the syringe needle and subsequently collected on the surface of the ePTFE membrane. Ultimately, the precursor ePTFE/fPTFE membrane was produced under the electrostatic attraction. In this context, six PTFE/PEO mass ratios, designated as M1–M6 (as listed in Table 1), had been selected for comparative analysis.

After drying in a vacuum oven at 60 °C for 12 h, the precursor composite membrane was sintered in a tube furnace (KSL-1200X, Kejing Auto Instrument Co.) at 380 °C in an air atmosphere (The reason for choosing 380 °C as the sintering temperature was explained through the results of thermal analysis included in Figs. S1–S3 in the electronic supplementary information, ESI). Subsequently, the furnace was gradually cooled to room temperature (about 20 °C) over a span of 10 h. After the sintering process, the ePTFE/fPTFE compounded membrane was separated from the PI film.

Similarly, using the formulation of M4 as a reference, the fPTFE layer with the average thickness of 35.2, 49.8, 76.3 and 102.4 μm was compounded with the ePTFE membrane by varying the electrospinning time to 2, 4, 6 and 8 h, respectively (Fig. S4 in ESI). Therefore, they were designated as M4-35.2, M4-49.8, M4-76.3 and M4-102.4, respectively.

### Characterization

The surface morphology of the fPTFE membrane was examined using a scanning electron microscope (SEM, NavoNano-SEM450) with an accelerating voltage of 5 kV. Before the observation, a fine layer of gold was coated onto the surface of each sample in a vacuum chamber. Fiber diameters were determined and counted using Image J software, with a total of 120 fibers and 200 micropores included in the analysis.

The average pore size and pore size distribution of the spun membranes were determined using a bubble-pressure method pore size analyzer (3H-2000 PB, Beijing, Bestech). Before testing, the dried compounded membrane samples were cut into 13 mm diameter discs and then fully wetted in a standard wetting solution with a surface tension of 16 dyn/cm.

https://doi.org/10.1007/s10118-024-3107-7

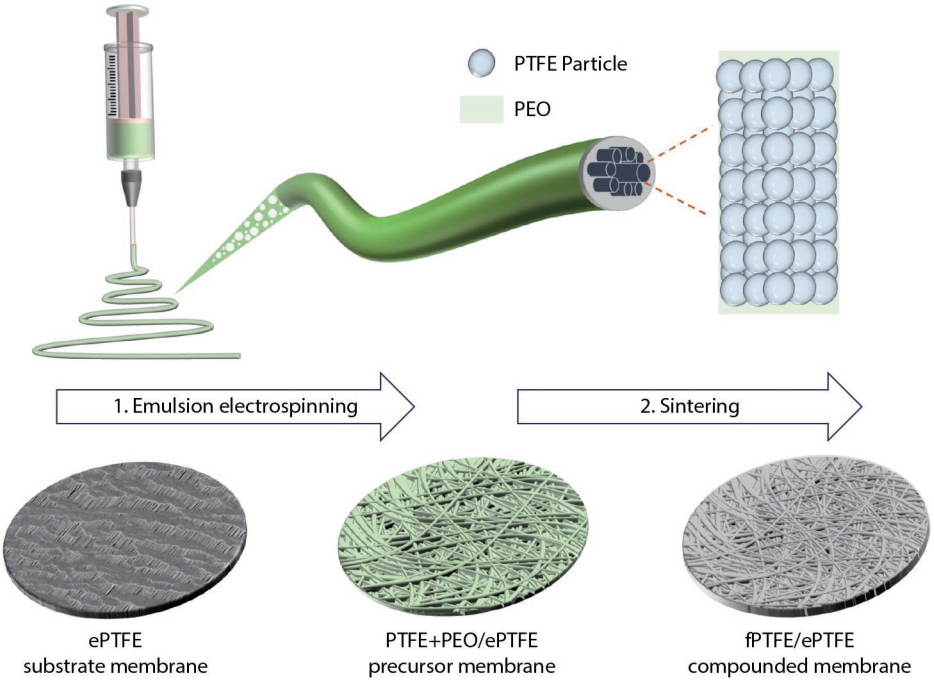


**Fig. 1** Schematic of the fabrication process of fPTFE/ePTFE compounded membrane. Step 1: Electrospinning of PTFE/PEO compounded nanofibers onto the ePTFE substrate; Step 2: The compounded membrane was sintered in the furnace to solidate the fPTFE layer and strengthen its adhesion to ePTFE substrate.

Five sets of data were tested for each sample to derive an average value. The porosity of membrane was determined gravimetrically, with *n*-butanol utilized as the wetting liquid to account for PTFE's hydrophobicity. Porosity measurement involved weighing the *n*-butanol liquid held within the membrane pores, in accordance with Eq. (1):[26]

$$\varepsilon = \frac{w_2 - w_1}{\rho V} \quad (1)$$

where $w_2$ corresponds to the weight (g) of the membrane after being infiltrated with *n*-butanol, $w_1$ corresponds to the weight (g) of the membrane before undergoing infiltration with *n*-butanol, $\rho$=0.8097 g/mL, which is the density of *n*-butanol, and $V$ denotes the volume of the sample membrane ($cm^3$).

Contact angles (CA) of both water and oil were measured using a CA20 instrument from the German data physics company. Each measurement utilized a single 3 μL droplet of either water or oil, and five CA values were recorded at various positions for each sample.

The mechanical properties of the compounded membranes were measured in the tensile direction using a SANSi CMT6503 Universal Testing Machine (China) at a speed of 50 mm/min at 25 °C. A minimum of five samples per film were tested to obtain an average of the tensile strength and elongation at break.

Surfactant-stabilized water-in-oil emulsions were created by combining 40 mL of chloroform, 2 mL of water, and 40 mg of span 80. The mixture was then sonicated at 40 kHz for 4 h. To demonstrate the stability of the as-prepared emulsion, it was left to stand for a week. The digital photographs and microscopic images included in Fig. S5 (in ESI) clearly present that the long-term emulsion appeared milky white without any visible separation and the latex particles were still uniformly dispersed in the medium, similar to that in the freshly prepared emulsion.

A Brinell's funnel with a sand core was used as the separation device, and the separated oil phase was collected in the funnel for subsequent analytical testing. The separation efficiency ($R$) can be calculated using Eq. (2):[27]

$$R = \left(1 - \frac{C_p}{C_0}\right) \cdot 100\% \quad (2)$$

where $C_0$ and $C_p$ represent the water content in the oil phase before and after separation, respectively, and the exact values were determined by a Karl Fischer moisture titrator (Mettler Toledo C20).[28]

The separation flux was calculated by Eq. (3):[29]

$$F = \frac{v}{s \cdot t} \quad (3)$$

where $v$ is the volume of liquid medium through the separation membrane (L), $s$ is the area of the effective separation area of the separation membrane ($m^2$), and $t$ is the time for the entire separation process to end (h).

Creep recovery tests were performed by using a Dynamic Mechanical Analyzer (DMA) (Q800, TA Instruments, New Castle, DE). The testing temperature was 25 °C. Samples with a width of 4 mm and a length of 20 mm were loaded into a tensile clamp inside the DMA oven. During each test, a constant stress of 2 MPa was maintained for 30 min to induce strain in the sample. Afterward, the stress was released, and the samples were given 1 h to recover from the strain.

## RESULTS AND DISCUSSION

### Microstructure and Interfacial Adhesion

The hierarchically compounded membrane of fPTFE/ePTFE, elu-

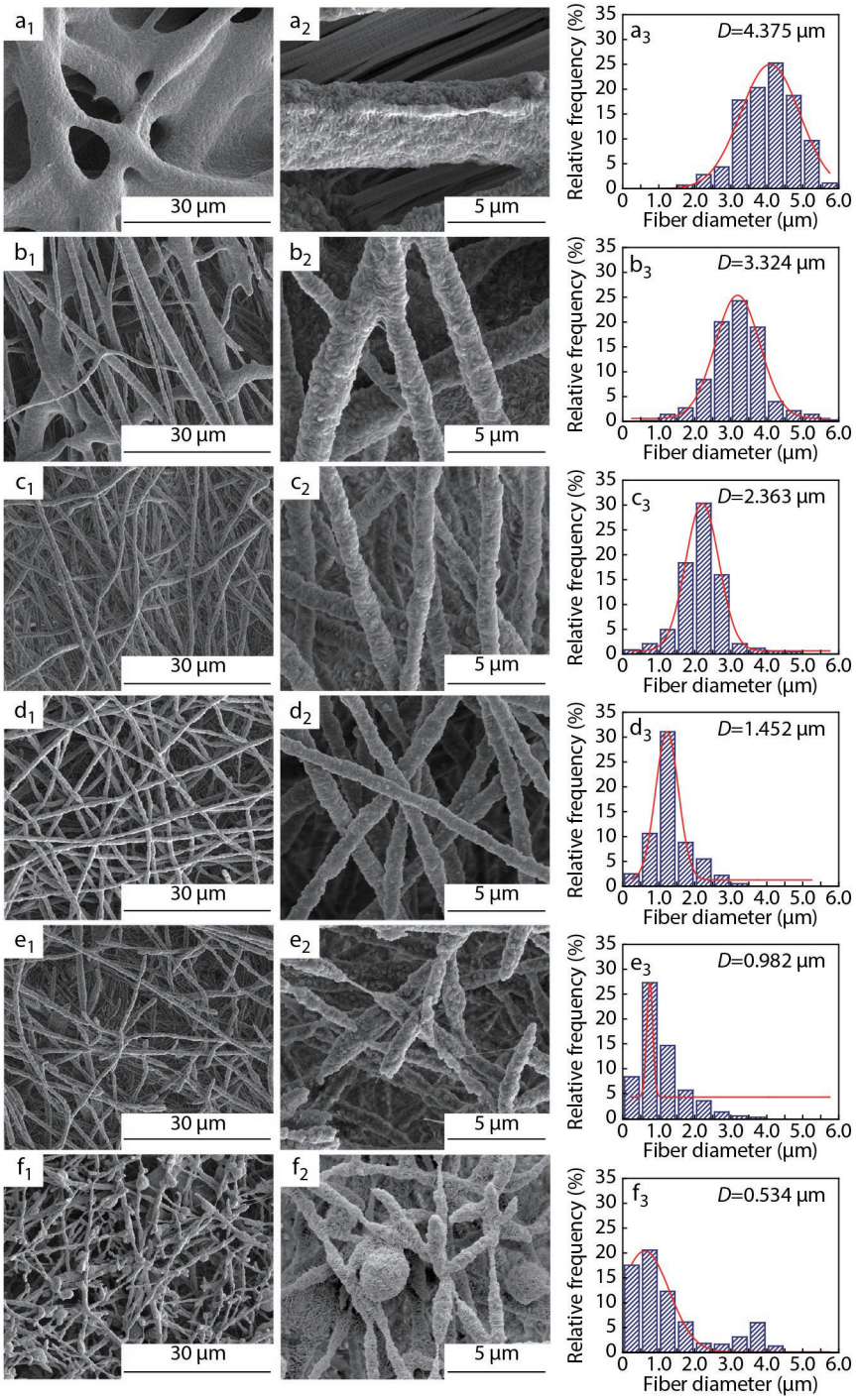


**Fig. 2** SEM images of electrospinning nanofiber membranes labeled as M1 to M6 ($a_1$–$f_1$), their corresponding magnified regions ($a_2$–$f_2$), and diameter distributions ($a_3$–$f_3$).

cidated in Fig. 1, is meticulously crafted through the electrospinning process of an fPTFE fibrous layer onto an ePTFE microporous substrate. The spinning solution primarily comprised a PTFE aqueous dispersion, dissolved with a specific quantity of PEO. Thus, the fibrous morphology of the fPTFE layer is significantly reliant on the formulation of the PTFE/PEO solution. The fibrous morphologies of the fPTFE membranes and the corresponding distribution of fiber diameters for each membrane are illustrated in Fig. 2. Notably, the average fiber diameter gradually diminishes from 4.375 μm in M1 to 0.534 μm in M6.

As PTFE is a polymer that is insoluble and infusible, a water-soluble PEO is utilized as a carrier to construct the fibrous architecture during the electrospinning process. Consequently, the resulting fibers exhibit an increase in diameter with the rise in the PEO mass ratio, a finding that concurs with antecedent research insights.

Moreover, it is noteworthy that an ultra-low concentration of PTFE or PEO may result in non-uniform distribution and dif-

https://doi.org/10.1007/s10118-024-3107-7

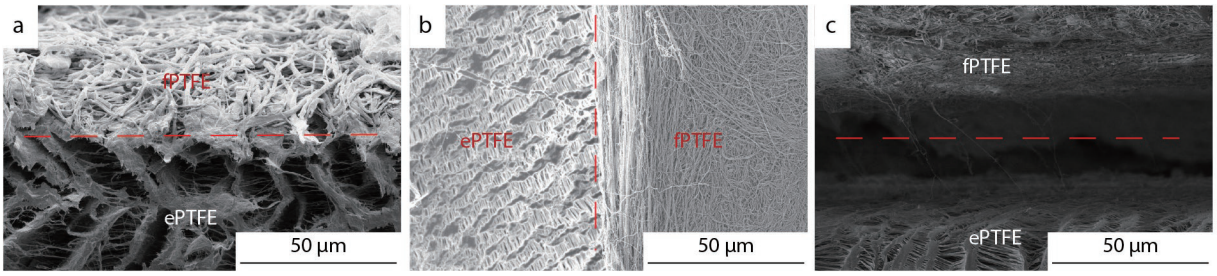


**Fig. 3** Microscopic observation of the interfaces of (a, b) M4 membrane by electrospinning a fPTFE membrane on an ePTFE substrate (a: side view of the interface; b: peeling off two layers from the interface), and (c) co-sintered membrane by placing a preprepared fPTFE membrane on an ePTFE substrate.

ferences in viscosity in localized parts, which can cause instability of the spinning solution during spraying. Specifically, the broader fiber diameter distribution observed in the image of M1 and the formation of intermittent bead-like structures observed in the image of M6 are associated with variations in the concentration of the spinning solution. As the SEM images for M5 and M6 reveal that numerous fibers have been fragmented into shorter segments, which can have a substantial adverse effect on the mechanical properties and selective separability of the membrane, only M1–M4 will be discussed in the subsequent analysis.

Furthermore, it is worth noting that in order to solidate the fPTFE layer and strengthen its adhesion to ePTFE substrate, a sintering process is performed on the compounded membranes at 380 °C, during which PTFE resins undergo melting, and the PEO component undergoes complete decomposition. The magnified cross-sectional image of M4 in Fig. 3(a) reveals that its interface is bonded tightly without any distinct gap. When the same compounded membrane is teared apart from the interface, it can even be seen from Fig. 3(b) that some fibers are still connected between fPTFE and ePTFE layers. For comparison, another hierarchical sample is produced by placing a piece of preprepared fPTFE membrane on an ePTFE substrate and then co-sintering them together at the same temperature without applying any extra force. As a result, such an unstressed stacking is easily to be peeled apart and the cross-sectional observation in Fig. 3(c) exhibits a visible gap at the layer interface. This indicates that the spinning solution can wet the ePTFE substrate, allowing the formed fibers to bind more tightly with the ePTFE after sintering.

## Pore Size and Porosity

The formulation of PTFE/PEO spinning solution also affects the porous structure of the as-prepared fPTFE layer. Quantitatively, Fig. 4 displays the pore size distribution and porosity of the compounded membranes labeled M1 to M4. As depicted in Fig. 4(a), the M1 membrane contains a wide distribution of pore size ranged from 5 μm to 20 μm and the average value is about 13.23 μm. With the reduction of PEO contents in the spinning solution, the pore size in the membrane becomes smaller and presents a narrower distribution. As shown in Fig. 4(d), the pore size distribution of the M4 membrane is primarily in the range of

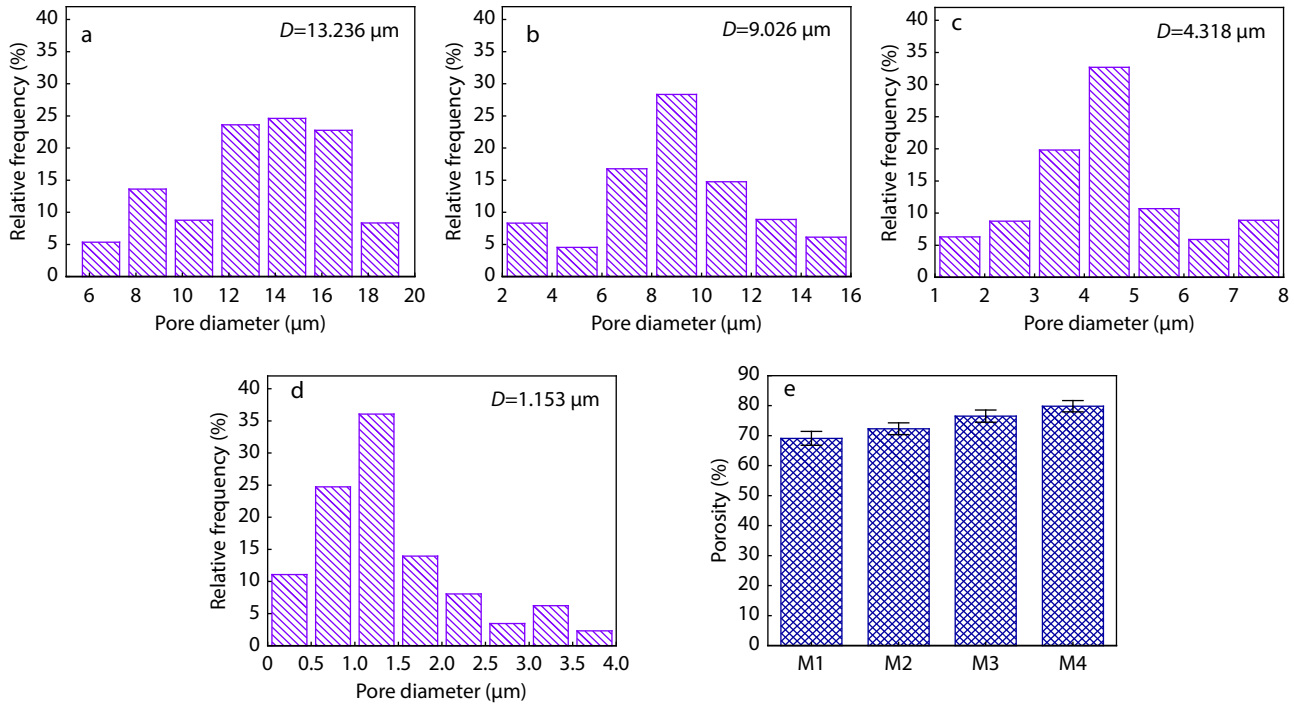


**Fig. 4** Pore size distribution of the membranes of (a) M1, (b) M2, (c) M3, (d) M4; (e) The comparison of their porosity.

https://doi.org/10.1007/s10118-024-3107-7

0 μm to 4 μm, with an average value of only 1.15 μm. This represents a reduction of approximately 91% compared to the M1 membrane. Furthermore, the porosity of the compounded membranes prepared with different PTFE/PEO formulations is compared in Fig. 4(e). It is clearly shown that the membrane containing the fPTFE layer with less PEO has a larger porosity, increased from 69.1% for M1 to 79.8% for M4. According to the structural observation in Fig. 2, an appropriate concentration of PEO can refine and homogenize the fibers in the fPTFE layer. This uniform fiber structure contributes to enhancing the stacking density of fibers during the spinning process. As a result, the pores in the M4 membrane own the smallest size, the most uniform distribution and the largest porosity, which are usually regarded as an ideal choice for the application of emulsion separation.

In addition to the ratio of PTFE to PEO, the fPTFE layer thickness tailored by controlling the electrospinning period also affects the pore structure of the compounded membranes. As presented in Figs. 5(a) and 5(b), it can be observed that with the thickening of fPTFE layer from 35.2 μm to 102.4 μm, the average pore size of the compounded membrane gradually decreases from 2.24 μm to 1.17 μm, whereas the porosity exhibits an increment from 58.4% to 80.2%. Such an opposite tendency can be explained by the gradual accumulation of PTFE fibers with the prolongation of electrospinning time, yielding smaller and denser pore structure.

## Superficial Wettability

The efficacy of the membrane in separation is intricately linked to its surface wettability. Consequently, water contact angle (WCA) and oil contact angle (OCA) are determined using deionized water and chloroform as test droplets, respectively. All measured outcomes are recorded in Fig. 6(a) for comparison. For the ePTFE membrane, the average WCA measures 126°, exceeding 90°, which indicates high hydrophobicity attributed to the low surface tension of PTFE. In the case of the fPTFE membrane (with the same formulation as the spun layer in M4), its WCA increases to about 149.8°, exhibiting a superhydrophobic characteristics. Considering the porous parameters outlined in Fig. 3, the average pore size of the M4 membrane is 1.25 μm and the porosity is 79.8%. In contrast, those of pristine ePTFE are only around 1 μm and 51% measured by the producer. It is widely acknowledged that the WCA on an air surface can reach as high as 180°. Therefore, the superior hydrophobicity of fPTFE should be originated from the higher proportion of air in the micropores, just like that happened on lotus leaves.[30,31] When the fPTFE and ePTFE membranes are hierarchically compounded together, the WCA on the surface of fPTFE side is almost constant, irrespective of the formulation of spinning solution. The opposite tendency of the pore size and porosity of the membrane from M1 to M4 may offset the influence of porous structure on WCA. Furthermore, the time dependent WCA was recorded by taking continuous photographs. As shown in Fig. 6(b), the contour of water droplet on the fPTFE side of M4 membrane barely alters for 60 min, thereby its WCA is basically maintained around 150°, indicating a long-term stability of the superhydrophobic characteristics.

On the other hand, the lipophilicity of the compounded membrane can be evaluated by dropping chloroform on the surface of fPTFE side to measure OCA. Taking the M4 membrane as an example, the photograph captured in Fig. 6(c) reveals that the oil droplet, upon landing on the surface, rapidly diffuses within 70 ms, indicating an OCA approaching 0°. This phenomenon can be explained by the surface lipophilicity, which forces the oil droplets to penetrate through the pores into the interior of the membrane.[16,32,33] In summary, these findings demonstrate that the fPTFE/ePTFE compounded membrane exhibits both super hydrophobicity and rapid oil infiltration, as evidenced by high WCA and remarkably low OCA values. This characteristic holds great potential for highly efficient oil-based water emulsions separation applications.

## Emulsion Separation Performance

The emulsion separation experiment was performed on a self-made device as illustrated in Fig. 7(a). The compounded membrane was positioned between the Buchner funnel and the flask. A surfactant-stabilized water-in-oil emulsion was prepared by mixing the water, chloroform and span 80 together, in which the chloroform acted as the oil phase and the span 80 was the surfactant. Subsequently, 15 mL of the prepared water-in-oil emulsion was introduced into the funnel (as shown in Fig. 7b). M4 was chosen as the representative membrane for separating water-in-oil emulsions due to its super hydrophobicity, extremely fast oil penetration, and its combination of small pore size and high porosity. The entire separation process occurred under the influence of gravity. It was evident that the colorless oil phase passed through the membrane into the flask, while the water phase was obstructed and gradually collected in the

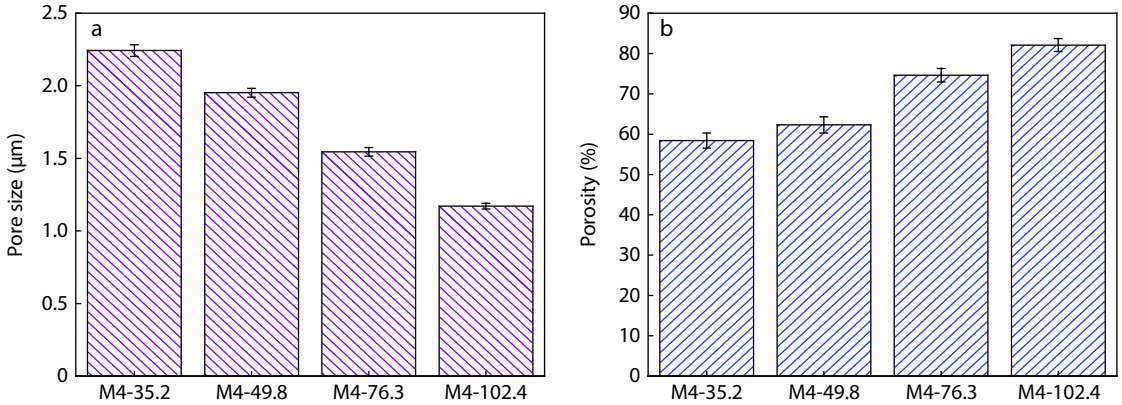


**Fig. 5** (a) The average pore size and (b) porosity of the compounded membrane with different thicknesses of fPTFE layer.

https://doi.org/10.1007/s10118-024-3107-7

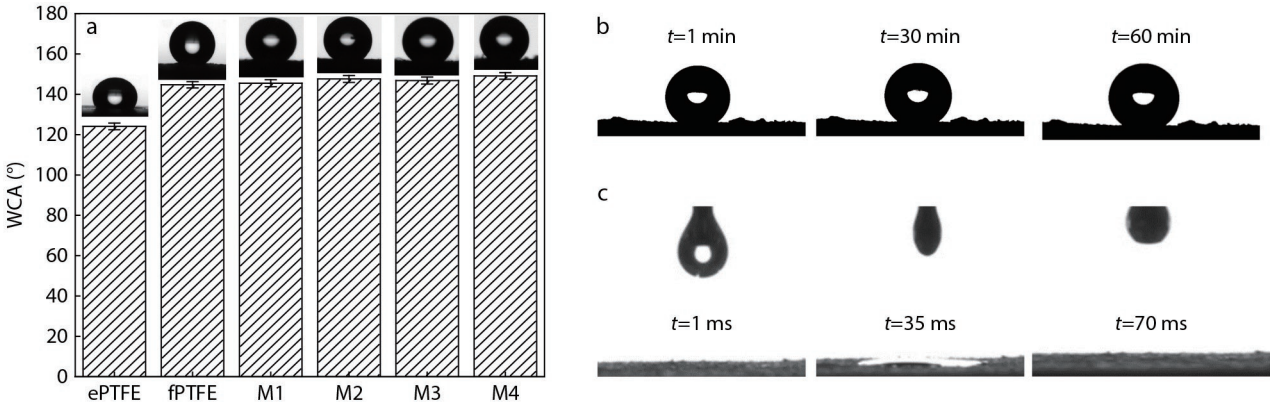


**Fig. 6** (a) Measured WCA values of ePTFE, fPTFE, and M1–M4 membranes; Spreading characteristics of (b) a water droplet and (c) an oil droplet on M4 membrane.


**Fig. 7** The process of the water-in-oil emulsion separation experiment: (a) initial state, (b) pouring the emulsion into the funnel, (c) carrying out the emulsion separation, (d) post-separation state.

upper tube (Fig. 7c). Furthermore, it was worth noting that the initially cloudy white emulsion turned remarkably clear after separation (Fig. 7d, Movie S1 in ESI), emphasizing the effectiveness of the unique bilayer structure in compounded membrane for separating water-in-oil emulsions.

To quantitatively evaluate the impact of the compounded membrane structure on water-in-oil emulsion separation performance, all samples, including ePTFE and M1–M4, underwent emulsion separation experiments using identical procedures and conditions. The separation efficiency ($R$) and separation flux ($F$) of each membrane were measured following Eqs. (2) and (3), presented in Fig. 8(a). Notably, ePTFE exhibits the lowest $R$ value at 54%, whereas the value for the compounded membranes gradually increase from 79.0% for M1 to 98.5% for M4. However, the separation fluxe shows the opposite trend, with the highest $F$ value of 208 $L{\cdot}m^{-2}{\cdot}h^{-1}$ for ePTFE, and a decrease in the $F$ value for the compounded membrane from 159 $L{\cdot}m^{-2}{\cdot}h^{-1}$ for M1 to 145 $L{\cdot}m^{-2}{\cdot}h^{-1}$ for M4. The variation in $R$ and $F$ values between ePTFE and the compounded membranes can be attributed to the relatively small WCA, lower porosity, and two-dimensional planar arrangement of the pore structure in ePTFE membranes.

It is well-established that the $R$ value is typically associated with the intrusion pressure ($P$) of a membrane, a relationship that can be determined using Eq. (4):[34]

$$P = 4\gamma\cos\theta/d \quad (4)$$

where $\gamma$ represents the oil-water interfacial tension, $\theta$ represents the WCA, and $d$ signifies the average pore size of the membrane. For all the compounded membrane samples from M1 to M4, the WCA remains relatively consistent, but there is a reduction in pore size, resulting in an increase in the $P$ value. This suggests that the emulsion would face greater resistance when passing through the separation membrane. Consequently, this contributes to the improved separation efficiency of membrane M4. Decreasing pore size leads to a longer separation duration of the media, resulting in an inverse correlation between $R$ value and $F$ value from M1 to M4. Encouragingly, in this study, the increase in $R$ value has a reduced effect on the $F$ value, which remained around 150 $L{\cdot}m^{-2}{\cdot}h^{-1}$ for the compounded membranes. This effect might be attributed to the observed increase in porosity from M1 to M4.

Furthermore, Fig. 8(b) depicts the influence of the fPTFE layer thickness on the separation performances of compounded membranes. With the thickening of fPTFE layer from 35.2 μm to 102.4 μm, the $R$ value increases from 66.8% to 98.8%, while the $F$ value decreases from 182 $L{\cdot}m^{-2}{\cdot}h^{-1}$ to 147 $L{\cdot}m^{-2}{\cdot}h^{-1}$, which can be explained by the gradual accumulation of PTFE fibers increasing the path for liquid to pass through the compounded membrane. It is worth noting that the $F$ values of the compounded membranes prepared in present work seem to be at a low level. It is well known that an electrospun layer is difficult to strongly adhere to a PTFE flat film without any microporous structure, due to the ul-

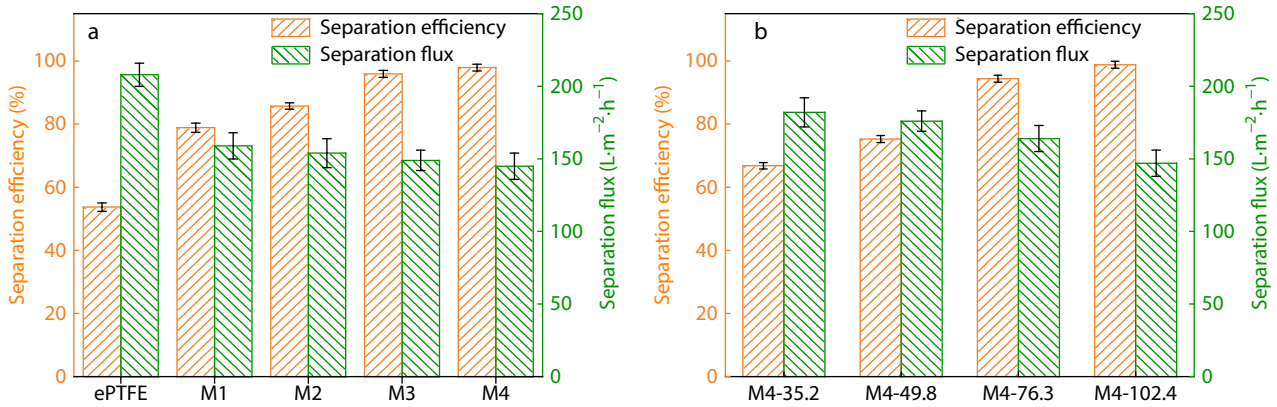


**Fig. 8** Separation efficiency and separation flux of the membranes of (a) ePTFE, M1, M2, M3, M4; (b) M4-35.2, M4-49.8, M4-76.3, and M4-102.4.

tralow surface energy. Herein, the flat film is replaced by an ePTFE microporous membrane, which consists of numerous stretched fibers. To demonstrate the applicability and feasibility of this strategy, a commercial ePTFE membrane with small pores consisting of short fibers (resulting in a low *F* value) was chosen to act as the electrospinning substrate.

To further explore the influence of distinct membrane structures on emulsion separation performance, the composition of the oil phase in the separated flask was analyzed with an optical microscope, and the results were displayed in Fig. 9. When the water-in-oil emulsion was fully separated by ePTFE membrane, the collected oil phase in the flask still appeared milky-white, and the microscopic image exhibited numerous small water droplets within the oil phase, which led to the light scattering. After separation using the compounded membrane, the oil phase became clear and transparent. Digital photograph results showed that the oil phase filtered through M1 still contained some water droplets, but their size and quantity were significantly reduced compared to the case of using the ePTFE membrane. By contrast, the oil filtered through M4 membrane nearly achieved a pure phase, with no visible water droplets in the field of view, signifying a sufficient separation of oil and water. This observation result was basically consistent with the tendency of the calculated separation efficiency. Hence, it is considered that appropriate pore size, elevated porosity, and a high degree of surface hydrophobicity are fundamental prerequisites for ensuring exceptional separation performance.

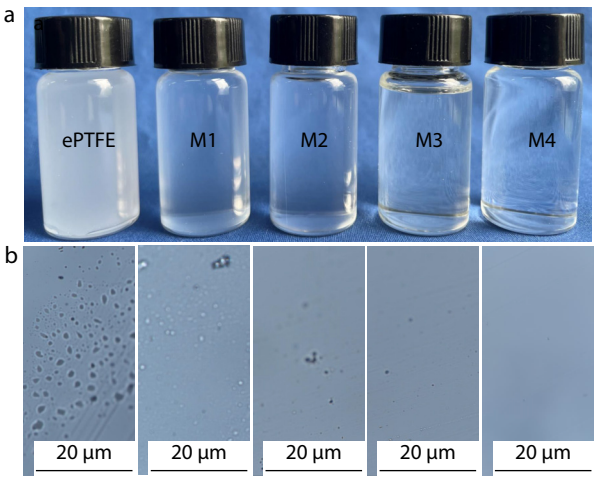


**Fig. 9** (a) Liquid collected in the flask after separation from these membranes; (b) Optical microscopic images of the collected liquid.

Fig. 10 illustrates the filtration process for both M1 and M4 membranes in the context of emulsion separation. Upon contact with the compounded membrane, the hydrophobic and lipophilic nature of the compounded membrane allows the oil, acting as a continuous phase, to swiftly pass through and occupy the surface cavities. In the case of M4 with smaller pore sizes (Fig. 10a), the composite interface effectively intercepts most water droplets, integrating them into the aqueous phase, ensuring efficient emulsion separation. Conversely, switching to the M1 membrane with relatively larger pore sizes (Fig. 10b) allows some tiny water droplets to traverse the pores driven by the oil phase, resulting in reduced separation efficiency.

In comparison, the performance of the compounded membranes for separating oil-in-water emulsion was investigated as well. An oil-in-water emulsion was prepared by adding 2 mL of chloroform to 40 mL of water containing 10 mg of Span 80. Fig. 11(a) depicts the digital photograph after pouring 15 ml emulsion into the separation device using M4 as the separation membrane. It can be observed that no liquid permeated through the membrane into the collection bottle below (Movie S2 in ESI) even after 3 h (Fig. 11b). This clearly demonstrates that the separation effect of the compounded membrane on the oil-in-water emulsion is different from that on the water-in-oil emulsion. This phenomenon is mainly attributed to the superhydrophobic and superoleophilic characteristics of the PTFE-based compounded membrane. In the water-in-oil emulsion, the oil phase as the continuous phase can quickly wet and pass through the separation membrane, achieving effective separation under the influence of gravity. However, in the oil-in-water emulsion, due to the superhydrophobic nature of the compounded membrane, the water phase as the continuous phase cannot wet the separation membrane. Relying solely on gravity makes it difficult for the compounded membrane to achieve effective separation of the oil-in-water emulsion.

## Reusability and Adaptability for Separation

The reusability stands as another crucial performance criterion for emulsion separation. In this regard, the water-in-oil emulsion was subjected to repeated separation using M4 for 12 cy-

https://doi.org/10.1007/s10118-024-3107-7

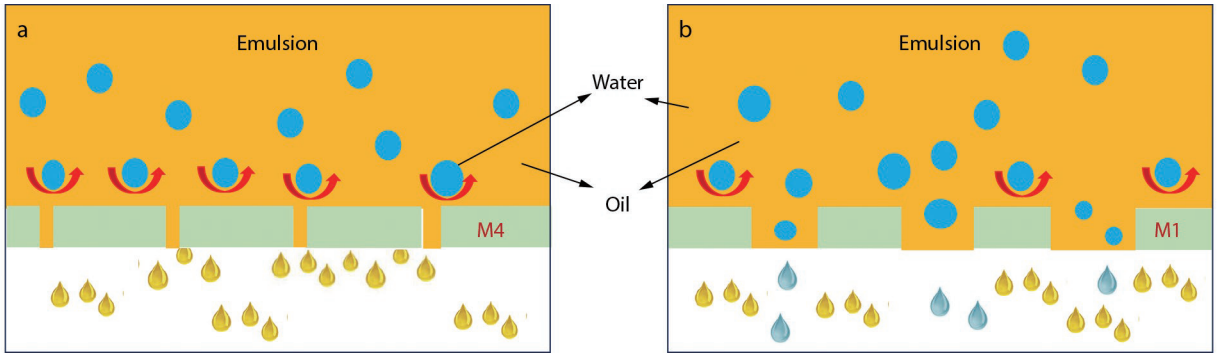


**Fig. 10** The emulsion separation process of (a) M4 and (b) M1 membranes.

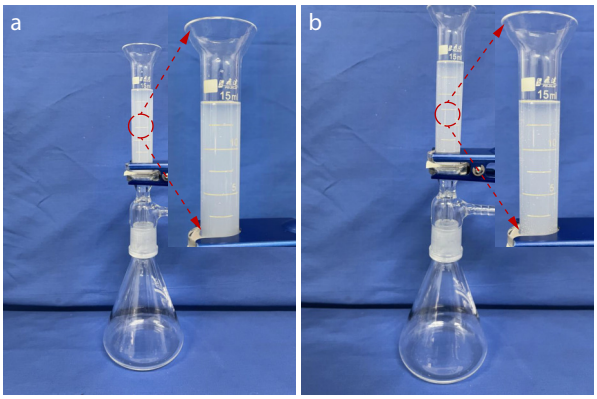


**Fig. 11** Separation of oil-in-water emulsion (a) before and (b) after 3 h separation by using the M4 membrane.

cles. Following each separation, the sample membrane was cleaned with ethanol and subsequently dried. Its reusability was then assessed by measuring the hydrophobicity of the membrane surface and the separation efficiency. As illustrated in Figs. 12(a) and 12(b), both the WCA and *R* values are maintained around 150° and 98% over 12 cycles, respectively, substantiating the exceptional reusability of the compounded membrane.

Furthermore, the application of the separation membrane is usually constrained by operating environment and conditions. Thereby, three kinds of harsh conditions, *i.e.*, strong acid (pH=1), strong alkali (pH=13) and high temperature (100 °C), were chosen in present study to assess their influence on the separation efficiency of the compounded membrane of M4. In the prelude to emulsion separation, each membrane received distinct durations of pre-treatment under the aforementioned three rigorous conditions. The results collected in Fig. 13 display that all the separation efficiency values measured are maintained around 98%, irrespective of the treat environment and period. It is regarded that remarkable corrosion resistance and high-temperature endurance of PTFE ensure the outstanding stability and adaptability of the compounded membranes.

## Mechanical Properties

The enduring operational lifespan of a separation membrane is predominantly dictated by its mechanical attributes. In present study, the mechanical properties of the compounded membrane may amalgamate the merits of fPTFE and ePTFE membranes, resulting in a more balanced comprehensive performance and a wider range of applications.

Fig. 14(a) presents the stress-strain curves of pristine ePTFE and fPTFE as well as their compounded membrane M4. In comparison to the ePTFE, which exhibits a distinct yield behavior and owns a tensile strength of 36.7 MPa, the fPTFE is almost linearly extended to a similar strain with the maximum strength of only 2.3 MPa. This notable distinction primarily arises from the disparate structures of fPTFE and ePTFE. The fibers of fPTFE are interconnected through latex particles, while ePTFE is constituted of a periodically oriented node-fiber structure. Unlike ePTFE, the molecular chains of fPTFE exhibit weak orientation and entanglement, rendering it less

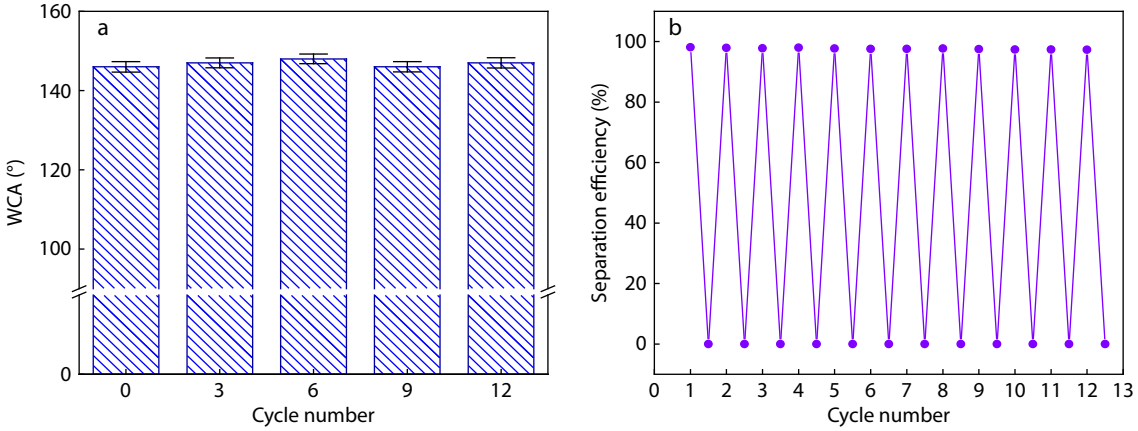


**Fig. 12** (a) Water contact angle (WCA) and (b) separation efficiency of M4 membrane after experiencing different cycle numbers.

https://doi.org/10.1007/s10118-024-3107-7

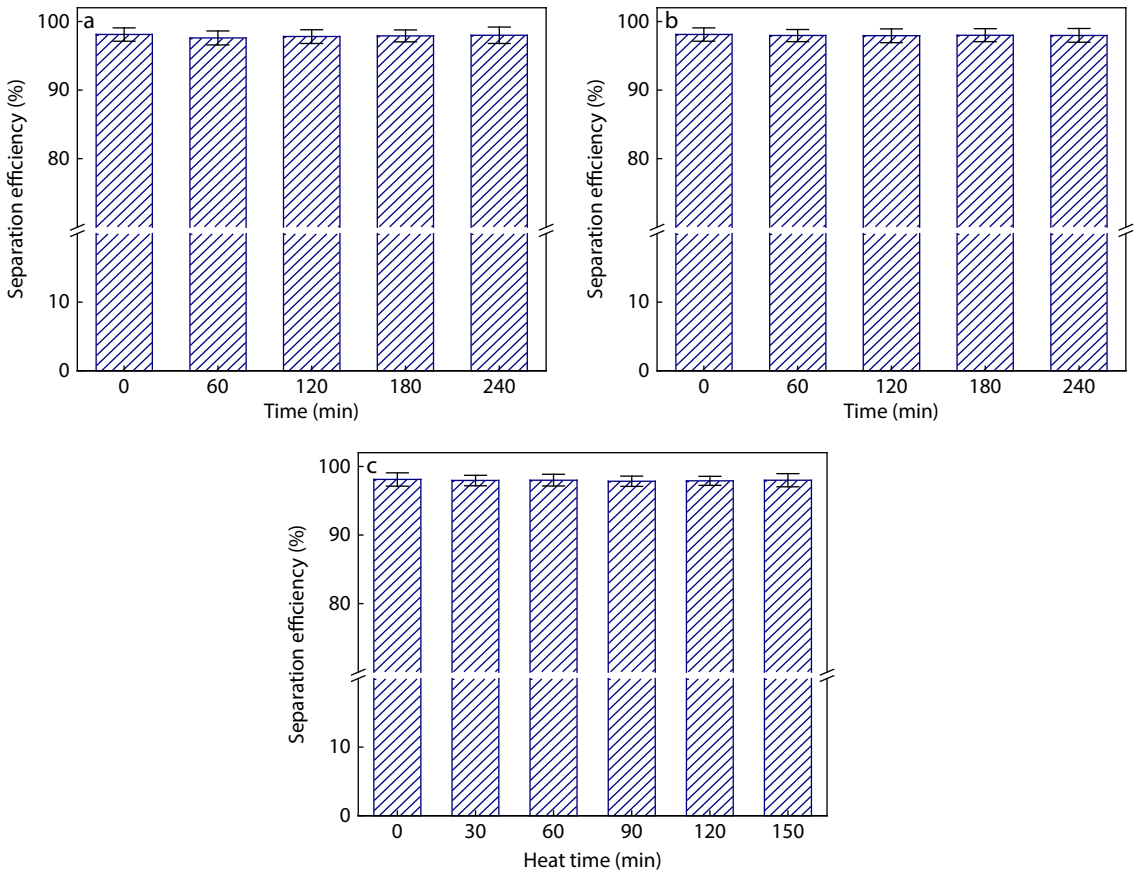


**Fig. 13** Separation efficiency of M4 membrane after being treated in different conditions: (a) pH=1, (b) pH=13, and (c) 100 °C.

resilient to substantial deformation stresses. When ePTFE and fPTFE are hierarchically compounded, the stress-strain curve of the bilayer membrane is intermediate between theirs and presents a similar yield behavior to that of ePTFE. For the M4 membrane, its tensile strength is 24.6 MPa, which is very close to the theoretical value of 25.7 MPa according to the classic parallel model.[35] This indicates that the mechanical behavior of the hierarchical compounding architecture is basically contributed by that of each layer in terms of their volume ratio.

Creep is another physical phenomenon characterizing the deformation when the constant stress is applied.[36] During creep, the time-independent elastic deformation first occurs, and then the time-dependent viscous strain gradually enlarges. When the stress is unloaded, both the elastic deformation and partial viscous deformation would recover at a specific time, and the permanent deformation would remain in the material.[37] In the last section, the ePTFE, fPTFE and M4 membranes were used to evaluate the influence of the hierarchical compounding on the creep resistance. In the creep stage (0–30 min), each membrane endured a constant stress of 2 MPa, followed by the instantaneous removal of stress to initiate the strain recovery stage (30–120 min). The strain-time curves recorded in Figs. 14(b)–14(d) are similar to those of other thermoplastics reported previously. It can be seen that the total strains in the creep stage are 4.5% for ePTFE and 72.0% for fPTFE, indicating that the latter one allows for a larger deformation by applying the same stress. In addition, the proportion of viscous strain in fPTFE is about 50%, whereas this value in ePTFE is 25%. Once the stress is removed, the fPTFE with a higher proportion of viscous strain has more permanent strain that cannot recover within the recorded time. This signifies that the fPTFE membrane has a poorer creep resistance than the ePTFE membrane. Such a dramatic distinction between these two membranes is effectively balanced by layering them together forming the M4 membrane, where the proportion of viscous and permanent strains are reduced to 30% and 38%, respectively, in comparison to those of the fPTFE membrane. Therefore, it is further substantiated that the hierarchical compounding plays a significant role in helping the fPTFE layer to resist irreversible deformation.

According to above results obtained in present study, it is evident that electro-spinning fPTFE on ePTFE substrate can effectively combine their performance advantages. As summarized in Fig. 15(a), the bilayer membrane exhibits fPTFE-like separation performance, achieving highly effective water-in-oil separation. On the other side, the same membrane also owns ePTFE-like mechanical and creep resistance, which can help fPTFE layer to resist irreversible deformation. Consequently, the hierarchical compounding endows the membrane with excellent comprehensive performances, which are proved to be competitive to other previously reported membranes applied for oil-water emulsion separation as collected in Fig. 15(b).[20,38–46]

https://doi.org/10.1007/s10118-024-3107-7

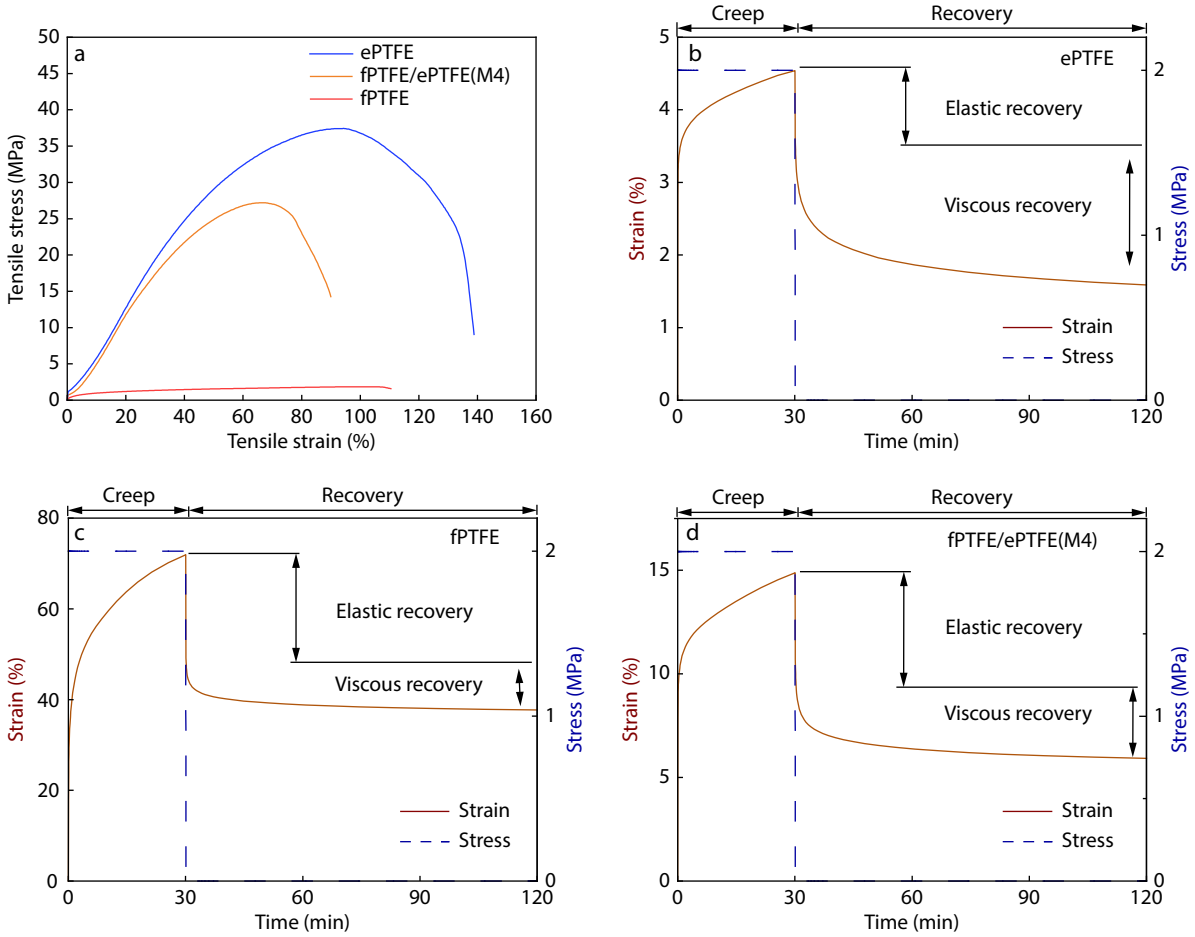


**Fig. 14** (a) Stress-strain curves of the membranes of ePTFE, fPTFE and M4; Creep recovery curves of (b) ePTFE, (c) fPTFE, and (d) M4 under 2 MPa tensile stress.

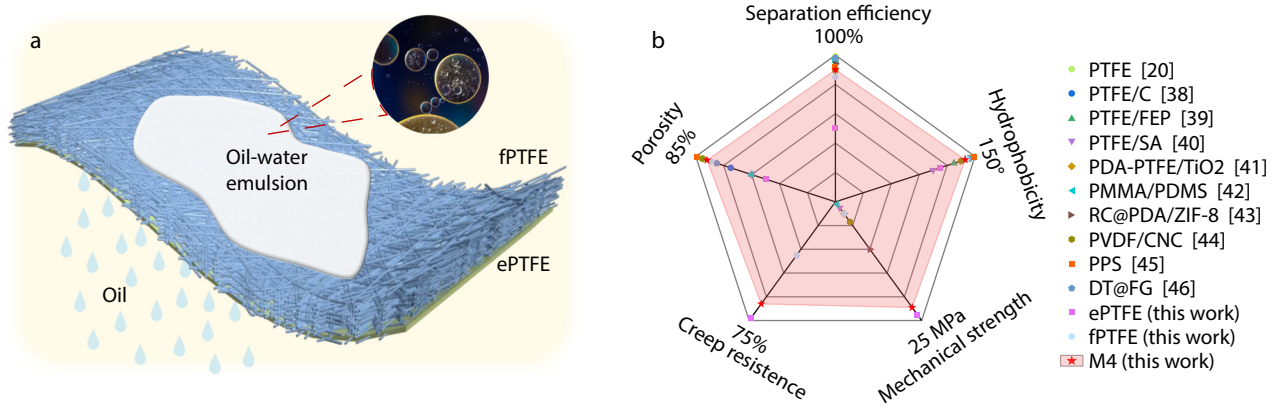


**Fig. 15** (a) Schematic of water-in-oil emulsion separation effect of M4 membrane; (b) Comparison of comprehensive performances between M4 and some of other previously reported membranes.

## CONCLUSIONS

The ePTFE/fPTFE bilayer membranes were fabricated by electrospinning PTFE fibrous layer on a microporous layer. The wetting of the PTFE/PEO spinning solution on the ePTFE substrate enabled the compounded membrane to possess a strong interfacial adhesion after sintering. The microstructure of the fPTFE layer was determined by the formulation of the spinning solution. Extremely low concentrations of either PTFE or PEO led to an instable spinning process, resulting in a wider distribution of fiber diameter or the formation of intermittent beaded structure. Within an optimal formulation range, a decrease in PEO concentration resulted in finer and more uniform fibers within the fPTFE layer. Simultaneously, the pore size decreased to 1.25 μm, while the porosity increased to 80%, resulting in a high WCA of 149.8° and rapid oil permeation. Benefited from the super-

https://doi.org/10.1007/s10118-024-3107-7

oleophilicity and superhydrophobicity, the compounded membrane demonstrated remarkable capabilities in separating water-in-oil emulsions, achieving a high separation efficiency approaching 100%. This performance was consistently maintained even after enduring 12 cycles of use and exposure to harsh conditions, including strong acid (pH=1), strong alkali (pH=12), or high-temperature (100 ℃) treatment. In addition, the hierarchical compounding effectively compensated for the drawbacks of low strength and poor creep resistance of the fPTFE layer, providing the bilayer membrane with high resistance to external forces. This attribute is crucial for ensuring its stable application in the emulsion separation.

## Conflict of Interests

The authors declare no interest conflict.

## Electronic Supplementary Information

Electronic supplementary information (ESI) is available free of charge in the online version of this article at http://doi.org/10.1007/s10118-024-3107-7.

## Data Availability Statement

The data that support the findings of this study are available from the corresponding author upon reasonable request. The author's contact information: shenjb@scu.edu.cn.

## ACKNOWLEDGMENTS

This work was financially supported by the National Natural Science Foundation of China (No. 52233003) and Project of Science and Technology Department of Sichuan Province (No. 2022JDJQ0023).

## REFERENCES

1 Sun, D. W.; Wang, Y. J.; Gao, J.; Liu, S. J.; Liu, X. L. Insights into the relation of crude oil components and surfactants to the stability of oily wastewater emulsions: influence of asphaltenes, colloids, and nonionic surfactants. *Sep. Purif. Technol.* **2023**, *307*, 122804.
2 Bhattacharyya, A.; Liu, L.; Lee, K.; Miao, J. H. Review of biological processes in a membrane bioreactor (MBR): effects of wastewater characteristics and operational parameters on biodegradation efficiency when treating industrial oily wastewater. *J. Mar. Sci. Eng.* **2022**, *10*, 1229.
3 Gao, G. H.; Xu, H. X.; Yu, X. H.; Jiang, L.; Wang, X. Q. Multifunctional PVDF nanofiber materials for high efficiency dual separation of emulsions and unidirectional water penetration. *Appl. Surf. Sci.* **2023**, *636*, 157808.
4 Hosseini, M. K.; Liu, L.; Hosseini, P. K.; Bhattacharyya, A.; Lee, K.; Miao, J. H.; Chen, B. Review of hollow fiber (HF) membrane filtration technology for the treatment of oily wastewater: applications and challenges. *J. Mar. Sci. Eng.* **2022**, *10*, 1313.
5 Kundua, P.; Mishra, I. M. Treatment and reclamation of hydrocarbon-bearing oily wastewater as a hazardous pollutant by different processes and technologies: a state-of-the-art review. *Rev. Chem. Eng.* **2019**, *35*, 73–108.
6 Wang, C.; Lu, Y. L.; Song, C.; Zhang, D. C.; Rong, F.; He, L. M. Separation of emulsified crude oil from produced water by gas flotation: a review. *Sci. Total Environ.* **2022**, *845*, 157304.
7 Baig, U.; Matin, A.; Gondal, M. A.; Zubair, S. M. Facile fabrication of superhydrophobic, superoleophilic photocatalytic membrane for efficient oil-water separation and removal of hazardous organic pollutants. *J. Clean. Prod.* **2019**, *208*, 904–915.
8 Khan, J. A.; Al-Kayiem, H. H.; Aleem, W.; Saad, A. B. Influence of alkali-surfactant-polymer flooding on the coalescence and sedimentation of oil/water emulsion in gravity separation. *J. Pet. Sci. Eng.* **2019**, *173*, 640–649.
9 Ariawan, A. B.; Ebnesajjad, S.; Hatzikiriakos, S. G. Paste extrusion of polytetrafluoroethylene (PTFE) fine powder resins. *Can. J. Chem. Eng.* **2002**, *80*, 1153–1165.
10 Dhanumalayan, E.; Joshi, G. M. Performance properties and applications of polytetrafluoroethylene (PTFE)–a review. *Adv. Comp. Hybrid Mater.* **2018**, *1*, 247–268.
11 Tomkovic, T.; Hatzikiriakos, S. G. Rheology and processing of polytetrafluoroethylene (PTFE) paste. *Can. J. Chem. Eng.* **2020**, *98*, 1852–1865.
12 Lee, C. H.; Johnson, N.; Drelich, J.; Yap, Y. K. The performance of superhydrophobic and superoleophilic carbon nanotube meshes in water-oil filtration. *Carbon* **2011**, *49*, 669–676.
13 Zheng, L. Z.; Li, H. Q.; Lai, X. J.; Huang, W.; Lin, Z. Y.; Zeng, X. R. Superwettable Janus nylon membrane for multifunctional emulsion separation. *J. Membr. Sci.* **2022**, *642*, 119995.
14 Cao, Y. Z.; Liu, N.; Zhang, W. F.; Feng, L.; Wei, Y. One-step coating toward multifunctional applications: oil/water mixtures and emulsions separation and contaminants adsorption. *ACS Appl. Mater. Interfaces* **2016**, *8*, 3333–3339.
15 Sutrisna, P. D.; Kurnia, K. A.; Siagian, U. W. R.; Ismadji, S.; Wenten, I. G. Membrane fouling and fouling mitigation in oil-water separation: a review. *J. Environ. Chem. Eng.* **2022**, *10*, 107532.
16 Shi, Y.; Hu, Y.; Shen, J.; Guo, S. Optimized microporous structure of ePTFE membranes by controlling the particle size of PTFE fine powders for achieving high oil-water separation performances. *J. Membr. Sci.* **2021**, *629*, 119294.
17 Feng, S.; Zhong, Z.; Wang, Y.; Xing, W.; Drioli, E. Progress and perspectives in PTFE membrane: preparation, modification, and applications. *J. Membr. Sci.* **2018**, *549*, 332–349.
18 Guo, Q.; Huang, Y.; Xu, M. D.; Huang, Q. L.; Cheng, J. X.; Yu, S. W.; Zhang, Y. X.; Xiao, C. F. PTFE porous membrane technology: a comprehensive review. *J. Membr. Sci.* **2022**, *664*, 121115.
19 Yu, S. W.; Huang, Q. L.; Cheng, J. X.; Huang, Y.; Xiao, C. F. Pore structure optimization of electrospun PTFE nanofiber membrane and its application in membrane emulsification. *Sep. Purif. Technol.* **2020**, *251*, 117297.
20 Wang, A.; Li, X.; Hou, T.; Lu, Y.; Zhou, J.; Zhang, X.; Yang, B. A tree-grapes-like PTFE fibrous membrane with super-hydrophobic and durable performance for oil/water separation. *Sep. Purif. Technol.* **2021**, *275*, 119165.
21 Tang, H.; He, J.; Hao, L.; Wang, F.; Zhang, H.; Guo, Y. Developing nanofiltration membrane based on microporous poly(tetrafluoroethylene) substrates by bi-stretching process. *J. Membr. Sci.* **2017**, *524*, 612–622.
22 Choi, K. J.; Spruiell, J. E. Structure development in multistage stretching of PTFE films. *J. Polym. Sci. B Polym. Phys.* **2010**, *48*, 2248–2256.
23 Liu, X.; Sun, J. Polymeric materials reinforced by noncovalent aggregates of polymer chains. *Aggregate* **2021**, *2*, 2766–8541.
24 Hao, X. M.; Zhang, H. C.; Guo, Y. H. Study of new protective clothing against SARS using semi-permeable PTFE/PU membrane. *Eur. Polym. J.* **2004**, *40*, 673–678.
25 Huang, H. Z.; Zhang, H. C. Hao, X. M.; Guo, Y. H. Study of a new novel process for preparing and co-stretching PTFE membrane

and its properties. *Eur. Polym. J.* **2004**, *40*, 667–671.
26 Matsuyama, H.; Teramoto, M.; Kudari, S.; Kitamura, Y. Effect of diluents on membrane formation *via* thermally induced phase separation. *J. Appl. Polym. Sci.* **2001**, *82*, 169–177.
27 Zhao, L.; Li, R.; Xu, R.; Si, D.; Shang, Y.; Ye, H.; Zhang, Y.; Ye, H.; Xin, Q. Antifouling slippery liquid-infused membrane for separation of water-in-oil emulsions. *J. Membr. Sci.* **2020**, *611*, 118289.
28 de Aquino, E. V.; Rohwedder, J. J. R.; Pasquini, C. A monosegmented-flow Karl Fischer titrator. *Talanta* **2007**, *71*, 1288–1293.
29 Jing, Y.; Zhang, L.; Huang, R.; Bai, D. Y.; Bai, H. W.; Zhang, Q.; Fu, Q. Ultrahigh-performance electrospun polylactide membranes with excellent oil/water separation ability *via* interfacial stereocomplex crystallization. *J. Mater. Chem. A* **2017**, *5*, 19729–19737.
30 Miller, M. W.; Parkinson, M.; Dato, A. Lotus-like water repellency of gas-phase-synthesized graphene. *ACS Mater. Lett.* **2022**, *4*, 995–1002.
31 Mukhopadhyay, R. D.; Vedhanarayanan, B.; Ajayaghosh, A. Creation of "rose petal" and "lotus leaf" effects on alumina by surface functionalization and metal-ion coordination. *Angew. Chem. Int. Ed.* **2017**, *56*, 16018–16022.
32 You, X. F.; Liao, Y.; Tian, M.; Chew, J. W.; Wang, R. Engineering highly effective nanofibrous membranes to demulsify surfactant-stabilized oil-in-water emulsions. *J. Membr. Sci.* **2020**, *611*, 118398.
33 Miao, W. Z.; Jiao, D. C.; Wang, C. Y.; Han, S. Q.; Shen, Q.; Wang, J.; Han, X. W.; Hou, T. C.; Liu, J. D.; Zhang, Y. T. Ethanol-induced one-step fabrication of superhydrophobic-superoleophilic poly(vinylidene fluoride) membrane for efficient oil/water emulsions separation. *J. Water Proc. Eng.* **2020**, *34*, 101121.
34 Cao, M. Y.; Li, K.; Dong, Z. C.; Yu, C. M.; Yang, S.; Song, C.; Liu, K. S.; Jiang, L. Superhydrophobic "pump": continuous and spontaneous antigravity water delivery. *Adv. Funct. Mater.* **2015,** *25*, 4114–4119.
35 Shen, J. B.; Wang, M.; Li, J.; Guo, S. Y.; Xu, S. X.; Zhang, Y. Q.; Li, T.; Wen, M. Simulation of mechanical properties of multilayered propylene-ethylene copolymer/ethylene 1-octene copolymer composites by equivalent box model and its experimental verification. *Eur. Polym. J.* **2009**, *45*, 3267–3279.
36 Desai, C. S.; Sane, S.; Jenson, J. Constitutive modeling including creep- and rate-dependent behavior and testing of glacial tills for prediction of motion of glaciers. *Int. J. Geomech.* **2011**, *11*, 465–476.
37 Gustafson, R. D.; McGaughey, A. L.; Ding, W. J.; McVety, S. C.; Childress, A. E., Morphological changes and creep recovery behavior of expanded polytetrafluoroethylene (ePTFE) membranes used for membrane distillation. *J. Membr. Sci.* **2019,** *584*, 236–245.
38 Zhang, Y.; Wu, J.; Cheng, J.; Zhao, Y.; Huang, Y.; Huang, Q. A simple and effective approach to regulate and control pore structure of electrospun PTFE nanofiber membrane. *Sep. Purif. Technol.* **2023**, *326*, 124848.
39 Guo, X.; Yao, Y.; Zhu, P.; Zhou, M.; Zhou, T. Preparation of porous PTFE/C composite foam and its application in gravity-driven oil-water separation. *Polym. Int.* **2022**, *71*, 874–883.
40 Huang, Y.; Xiao, C.; Huang, Q.; Liu, H.; Guo, Z.; Sun, K. Robust preparation of tubular PTFE/FEP ultrafine fibers-covered porous membrane by electrospinning for continuous highly effective oil/water separation. *J. Membr. Sci.* **2018**, *568*, 87–96.
41 Yu, X.; Zhu, W.; Li, Y.; Zhu, W.; Chen, X.; Hao, H.; Yu, M.; Huang, Y. Dual-bioinspired fabrication of Janus micro/nano PDA-PTFE/$TiO_2$ membrane for efficient oil-water separation. *Sep. Purif. Technol.* **2024**, *330*, 125201.
42 Tsai, Y. T.; Maggay, I. V.; Venault, A.; Lin, Y. F. Fluorine-free and hydrophobic/oleophilic PMMA/PDMS electrospun nanofibrous membranes for gravity-driven removal of water from oil-rich emulsions. *Sep. Purif. Technol.* **2021**, *279*, 119720.
43 Xie, A.; Cui, J.; Yang, J.; Chen, Y.; Lang, J.; Li, C.; Yan, Y.; Dai, J. Dual superlyophobic zeolitic imidazolate framework-8 modified membrane for controllable oil/water emulsion separation. *Sep. Purif. Technol.* **2020**, *236*, 116273.
44 Wang, X.; Cheng, W.; Wang, D.; Ni, X.; Han, G. Electrospun polyvinylidene fluoride-based fibrous nanocomposite membranes reinforced by cellulose nanocrystals for efficient separation of water-in-oil emulsions. *J. Membr. Sci.* **2019**, *575*, 71–79.
45 Kou, X. H.; Han, N.; Zhang, Y. Q.; Tian, S. W.; Li, P. K.; Wang, W.; Wu, C.; Li, W.; Yan, X. H.; Zhang, X. X. Fabrication of polyphenylene sulfide nanofibrous membrane *via* sacrificial templated-electrospinning for fast gravity-driven water-in-oil emulsion separation. *Sep. Purif. Technol.* **2021**, *275*, 119124.
46 Li, J.; Huang, S. Y.; Zhang, L. L.; Zhao, H. R.; Zhao, W. K.; Yuan, C. Z.; Zhang, X. M. One-pot *in-situ* deposition toward fabricating superhydrophobic fiberglass membranes with composite microstructure for fast water-in-oil emulsions separation. *Sep. Purif. Technol.* **2023**, *313*, 123480.

https://doi.org/10.1007/s10118-024-3107-7